Audio Engineering Society

Convention Paper 9501

Presented at the 140th Convention
2016 June 4–7, Paris, France

Metrics for Constant Directivity

Rahulram Sridhar, Joseph G. Tylka, and Edgar Y. Choueiri

3D Audio and Applied Acoustics Laboratory, Princeton University, Princeton, NJ, 08544, USA

Correspondence should be addressed to Rahulram Sridhar (rahulram@princeton.edu)

ABSTRACT

It is often desired that a transducer have a polar radiation pattern that is invariant with frequency, but there is currently no way of quantifying the extent to which a transducer possesses this quality (often called "constant directivity" or "controlled directivity"). To address this problem, commonly-accepted criteria are used to propose two definitions of constant directivity. The first, stricter definition, is that the polar radiation pattern of a transducer must be invariant over a specified frequency range, whereas the second is that the directivity index (i.e., the difference, in dB, between the on-axis frequency response and the average response over all directions), must be invariant with frequency. Furthermore, to quantify each criterion, five metrics are derived: 1) Fourier analysis of contour lines (i.e., lines of constant sensitivity over frequency and angle), 2) directional average of frequency response distortions, 3) distortion thresholding of polar responses, 4) standard deviation of directivity index, and 5) cross-correlation of polar responses. These five metrics are computed using measured polar radiation data for four loudspeakers. The loudspeakers are then ranked, from most constant-directive to least, according to each metric, and the rankings are used to evaluate, by comparison with each other and with a predetermined "correct" ranking, each metric's ability to quantify constant directivity. Results show that all five metrics are able to quantify constant directivity according to the criterion on which each is based, while only two of them, metrics 4 and 5, are able to adequately quantify both proposed definitions of constant directivity.

1 Introduction

Many applications in audio benefit from transducers (or transducer arrays) whose directional characteristics do not vary with frequency. For example, in live sound reinforcement, it is often desirable for each loudspeaker to cover a certain region of the audience. Consequently, the loudspeaker's *coverage angle* should be constant over its usable frequency range so that no part of the audience lacks any part of the frequency spectrum [1]. Also, microphone arrays used for beamforming often attempt to isolate and capture sounds (of all frequencies) from a certain direction (or region), which requires that the spatial selectivity of the array be frequency-independent [2, 3].

Many transducer manufacturers claim to achieve "constant directivity," suggesting that the transducer's directional characteristics, or some aspect thereof, are independent of frequency (at least over some frequency range). However, there exists no standard measure of the degree to which a transducer exhibits constant directivity, thereby making it impossible to evaluate these claims and compare supposed constant-directive devices. Part of the problem is that constant directivity is often imprecisely and/or implicitly defined, whereby, for example, the polar radiation of an "ideal" constant-directive loudspeaker is plotted alongside a real loud-

speaker's polar radiation pattern [4]. The reader is then left to visually judge to what degree that loudspeaker's radiation pattern qualifies as constant-directive, a process which is highly subjective and prone to error. In an attempt to resolve any ambiguity surrounding this topic, we seek a formal and quantifiable definition of constant directivity.

1.1 Background and Previous Work

In this paper, we refer to the *directivity* of a transducer as, generally, the extent to which its sensitivity (radiated acoustic power for loudspeakers) is biased toward a given direction. Several metrics exist to quantify directivity, the most well-known of which are the beamwidth (or the coverage angle for loudspeakers) and the directivity factor (or directivity index when expressed in dB) [5]. The coverage angle is typically defined as the angle between the -6 dB points of the main lobe [5]. As the name implies, this metric quantifies the region of space in which the radiation is largely uniform. The *directivity factor*, also known as the directional gain, is given by the ratio between the power radiated on-axis (or along any given reference axis) and the average power radiated over all directions [6]. Methods to calculate the directivity factor from a finite set of measured data have been developed [7, 8, 9, and references therein]. Another directivity metric, called the "directivity figure of merit," was proposed by Davis [10] and combines the directivity factor and the coverage angle to quantify the efficiency with which the radiated power is concentrated within the coverage angle.

Unlike for directivity, no metrics exist for constant directivity, likely due to a lack of a standardized, quantifiable definition of the term. For example, White [1] defines constant directivity as having a constant coverage angle over a wide frequency range. Geddes [11], on the other hand, defines constant directivity as having identical (up to a scaling factor) polar response curves (presumably over a wide frequency range). However, in a later publication, Geddes [4] states that no universal definition for constant directivity exists, and so to illustrate constant directivity, one should simply publish polar response data, implying that a purely visual assessment of the data is sufficient to determine to what extent a transducer is constant-directive. In the spirit of the work done to develop directivity metrics, this work attempts to address the lack of both a standardized definition of, and quantitative metrics for, constant directivity.

1.2 Objectives and Approach

It is the primary objective of this work to develop metrics for constant directivity that can be used to objectively evaluate and compare transducers. Additionally, it is the goal of this work to establish a precise definition for constant directivity, and subsequently determine which metric(s) most effectively quantify that definition.

To these ends, we first identify, in Section 2, various criteria for constant directivity, which are used to propose two definitions of the term. We then derive, in Section 3, metrics designed to quantify each criterion. In Section 4, these metrics are computed using a database of loudspeaker polar radiation measurements.[1] Finally, in Section 5, a subset of these loudspeakers are ranked, from most constant-directive to least, according to each metric, and the rankings are qualitatively compared with each other and with a predetermined ranking based on a visual analysis of plots of the loudspeakers' polar radiation patterns. In Section 6, we identify those metrics that best quantify our proposed definitions for constant directivity.

2 Defining "Constant Directivity"

Before we derive metrics which quantify constant directivity, we must first define what it means for a transducer to exhibit constant directivity. It is important to note that, at this point, the term "constant directivity" should not be considered synonymous with "directivity which is constant," as the term "directivity" is already defined, while "constant directivity" is not.

I. **Uniformly horizontal contour lines**
For a loudspeaker, a contour plot shows the loudspeaker's output level in dB, normalized by the on-axis output, as a function of both frequency and angle, with contours drawn at specific levels (e.g., -18 to 0 dB in increments of 3 dB). Based on such a plot, our first criterion for constant directivity is

[1] This database consists of 26 loudspeakers and is available online from the 3D Audio and Applied Acoustics Laboratory at Princeton University: `http://www.princeton.edu/3D3A/Directivity.html`

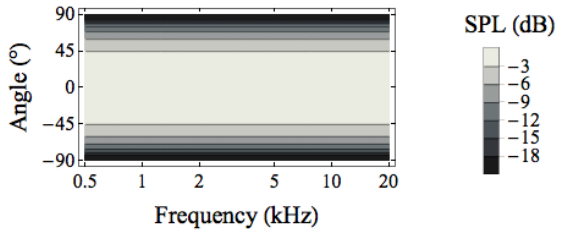

Fig. 1: Contour plot of an ideal constant directivity transducer according to criterion I.

that an ideal constant directivity transducer should have a contour plot in which all contour lines are perfectly horizontal [4], such as the contour plot shown in Fig. 1.

II. **Direction-independent frequency response**
In studio or live sound settings, it is often desirable for a listener at an off-axis position to receive the same spectral content as one on-axis [1], although perhaps at a lower overall level. From this motivation, our second criterion is that an ideal constant directivity transducer should have a frequency response at any off-axis position that is identical to its on-axis frequency response, ignoring any difference in overall level.

III. **Frequency-invariant "directivity"**
Finally, it appears clear from the term "constant directivity" that some aspect of the transducer's directional characteristics should be invariant with frequency. As defined in Section 1.1, "directivity" describes the directional bias in a transducer's sensitivity, a quality which is quantified by metrics such as the directivity factor and the coverage angle. By this definition, and a literal reading of the term "constant directivity," our third criterion is that an ideal constant directivity transducer should have a directivity (or some metric thereof) which is invariant with frequency [1]. However, fulfillment of this criterion is insufficient to guarantee fulfillment of the two previous criteria, as the directivity metrics reduce the full specification of the polar radiation pattern(s) to a single number (or spectrum). Consequently, to guarantee fulfillment of all three criteria, we must turn to an alternative, and more strict, third criterion: that an ideal constant directivity transducer should have polar radiation patterns that are unchanged (ignoring any differences in overall level) with frequency [11].

In view of these three criteria, we propose the following definition for constant directivity: *A transducer is said to exhibit constant directivity, over a specified frequency range, if and only if its polar radiation patterns are invariant in that range.* Furthermore, a transducer is said to be more (or less) constant-directive than another transducer, if the variations in the first transducer's polar radiation patterns are less (or more) extreme than those of the second transducer.

It is worth mentioning that, for some applications, the more lenient version of the third criterion may be appropriate. For example, in some beamforming applications, variations in polar radiation patterns may be tolerable provided that the directional gain (directivity factor) is constant over a specified range of frequencies. Consequently, we propose a second, more lenient definition for constant directivity: *A transducer is said to exhibit constant directivity, over a specified frequency range, if and only if its directivity factor (index) is invariant with frequency in that range.*[2]

3 Proposed Constant Directivity Metrics

We now derive five metrics for constant directivity, each of which is based on one of the preceding criteria. The first metric is based on criterion I, and quantifies the extent to which the contour lines are horizontal. The second and third metrics are both based on criterion II, and quantify the distortions in shape of a transducer's frequency responses at off-axis positions compared to its on-axis frequency response. The last two metrics are based on the two versions of criterion III, and quantify the extent to which a transducer's directivity is constant with frequency (metric 4) and the similarity of the transducer's polar responses (metric 5).

3.1 Metric 1: Fourier Analysis of Contour Lines

For this metric, we express the relative SPL (i.e., SPL normalized by the on-axis SPL) as a function of frequency (denoted by the index k) and for each angle

[2] Alternate versions of this definition can be generated by replacing the directivity factor with another directivity metric, e.g., the coverage angle.

(denoted by the index n) in a given polar orbit (e.g., horizontal or vertical), in dB, by

$$20\log_{10}\frac{|H_n[k]|}{|H_0[k]|},$$

where $n=0$ corresponds to 0° (on-axis), and H_n is the n^{th} frequency response of the transducer. We use these spectra to generate a contour plot in which the contour lines are black and all spaces between contour lines are white. The contours are drawn on a logarithmic frequency scale over a given frequency range, over a specified range of angles (e.g., −90° to 90° or 0° to 360°), and with a specified set of contour levels. Using Mathematica, the plot is then converted to a grayscale raster graphics image of width V and height U (in pixels). These data are stored in a U-by-V real matrix, $\mathbf{X}$, with elements $x_{u,v}\in[0,1]$, where contour lines are represented by non-zero values of x and the spaces between contours are represented by zeros.

We then compute the discrete Fourier transform (DFT) along each row of the matrix to yield a complex-valued U-by-V matrix, $\mathbf{Y}$, with elements $y_{u,v}$. The values in the first column of $\mathbf{Y}$ represent the DC components of each row of $\mathbf{X}$. In the ideal case, where all contours are perfectly horizontal, the only non-zero values of $\mathbf{Y}$ will exist in the first column (i.e., $y_{u,v\neq 0}=0$). In less ideal cases, where the contours are not perfectly horizontal, some of the signal energy in each row of $\mathbf{X}$ will spread to frequencies other than DC, resulting in non-zero values in more than just the first column of $\mathbf{Y}$. Consequently, we define our metric as the percentage of the total energy of $\mathbf{Y}$ that exists in the first column, given by

$$\varepsilon = 100\times\frac{\sum_{u=0}^{N-1}|y_{u,0}|^2}{\sum_{u=0}^{N-1}\sum_{v=0}^{M-1}|y_{u,v}|^2}. \tag{1}$$

The result is a strictly positive number $\varepsilon\in(0,100]$, where a value of $\varepsilon=100\%$ indicates that each row of $\mathbf{X}$ is a constant value (i.e., either it contains a complete contour or it does not) and represents a perfectly constant-directive transducer. A value of $\varepsilon=0\%$ is not possible because that would indicate that no row of $\mathbf{X}$ has any DC energy (i.e., no contours exist).

3.2 Metric 2: Directional Average of Frequency Response Distortions

We first define the *distortion spectrum* as

$$D_n[k]=\sqrt{\frac{P_n[k]}{\overline{P_n}}\Big/\frac{P_0[k]}{\overline{P_0}}}, \tag{2}$$

where $\overline{P_n}$ is the logarithmically-weighted average (see Appendix for details) of the n^{th} power spectrum (with $n=0$ corresponding to on-axis), $P_n[k]=|H_n[k]|^2$, over a given frequency range.

When the logarithm is taken, the distortion spectrum becomes the difference between the n^{th} frequency response and the on-axis response, minus the change in overall (average) level. Therefore, this spectrum shows the change in the *shape* of the frequency response, rather than the total change, for a given direction, isolating any change in tonality from any overall decrease in level which may occur at off-axis positions.

We then compute the *absolute* distortion spectrum, given by

$$E_n[k]=10^{|\log_{10}D_n[k]|}, \tag{3}$$

so that relative peaks and notches contribute equally to the result. These spectra are now averaged over all directions within a given region of space (e.g., ±30° horizontal, ±10° vertical), hereafter referred to as the "listening window," to yield the *listening window distortion spectrum*, given by

$$C_{\text{LW}}[k]=\sqrt{\frac{\sum_{n=0}^{N-1}w_n|E_n[k]|^2}{\sum_{n=0}^{N-1}w_n}}, \tag{4}$$

where the weights w_n correspond to the surface area of the unit sphere represented by each measurement and N is the number of measurements in the specified listening window. In particular, we use the same weights as used to calculate the directivity index from a finite set of measurements, as described in Section 3.4. This spectrum may be further averaged over frequency to yield a single number, the *average listening window distortion*, $\overline{C_{\text{LW}}}$, given by the square-root of the logarithmic average of $|C_{\text{LW}}[k]|^2$, and typically expressed in dB (i.e., $20\log_{10}\overline{C_{\text{LW}}}$).

Similarly, the *listening window response* is calculated as[3]

$$H_{\text{LW}}[k]=\sqrt{\frac{\sum_{n=0}^{N-1}w_n|H_n[k]|^2}{\sum_{n=0}^{N-1}w_n}}. \tag{5}$$

[3]This average response over the listening window is sometimes called the "direct sound" [12].

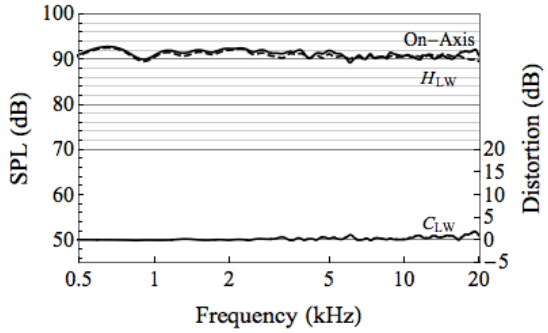

(a) Loudspeaker C: $\overline{C_{LW}} = 0.38$ dB

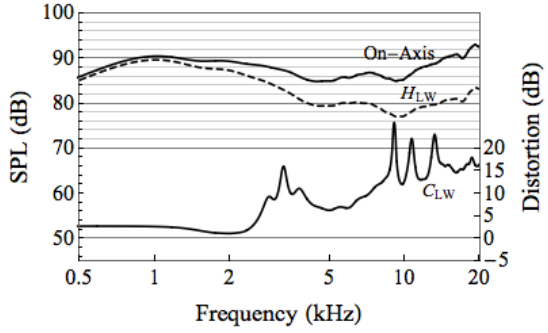

(b) Loudspeaker D: $\overline{C_{LW}} = 12.36$ dB

Fig. 2: Plots of H_0 (on-axis), H_{LW}, and C_{LW}, in dB, for two loudspeakers, C (top panel) and D (bottom).

To visualize this metric, we plot the power spectra for H_0, H_{LW}, and C_{LW}, in dB. Two such plots are shown in Fig. 2 for two loudspeakers, C and D (described in Table 1). Loudspeaker C is more constant-directive than loudspeaker D within a $\pm 30^\circ$ (horizontally, away from on-axis) listening window because of the larger dB values that the listening window distortion spectrum, C_{LW}, reaches in the case of loudspeaker D. The greater separation between the H_0 (on-axis) and H_{LW} spectra observed for this loudspeaker is also an indication of the same.

3.3 Metric 3: Distortion Thresholding of Polar Responses

For this metric, we use the same absolute distortion spectra defined in Eq. (3) for metric 2 to determine a frequency-dependent region of each polar orbit (i.e., horizontal and vertical) within which the distortion is below a specified threshold (e.g., 3 dB). For a given frequency index k, we search, up to 90° on either side of on-axis, for the pair of angles, $\theta_-[k]$ and $\theta_+[k]$, nearest to on-axis between which the distortion never exceeds the threshold. We then compute the frequency-dependent *constant-directive (CD) coverage angle*, $\theta_{CD}[k]$, given by $\theta_{CD} = \theta_+ - \theta_-$. This angle is then averaged logarithmically over a specified frequency range to yield an average CD coverage angle, $\overline{\theta_{CD}}$. Larger values of θ_{CD} indicate a wider region of tolerable distortion.

Label	Description
A	Active two-way studio monitor
B	Three-way "constant directivity" dipole loudspeaker
C	Active three-way concentric studio monitor
D	Electrostatic loudspeaker with transmission line woofer

Table 1: Descriptions of the four loudspeakers used in this work.

To visualize this metric, we plot $\theta_-[k]$ and $\theta_+[k]$, as shown in Fig. 3 for the same two loudspeakers C and D, and shade the region between them to highlight the angular range within which the distortion never exceeds 3 dB. We also indicate the averages of $\theta_-[k]$ and $\theta_+[k]$ by the dashed lines on either side of on-axis, the difference between which is equal to the average CD coverage angle, $\overline{\theta_{CD}}$. The larger value of $\overline{\theta_{CD}}$ for loudspeaker C compared to loudspeaker D indicates that the former exhibits a wider region within which the distortion is at most 3 dB, and is therefore more constant-directive.

Finally, using the frequency-dependent CD coverage angles from both horizontal and vertical polar orbits (indicated by the superscripts "H" and "V", respectively), we also compute a CD coverage solid angle, $\Omega_{CD}[k]$, given (in sr) by

$$\begin{aligned}\Omega_{CD}[k] = &\sin^{-1}\left(\sin(\theta_+^H[k])\sin(\theta_+^V[k])\right)\\ &+\sin^{-1}\left(\sin(-\theta_-^H[k])\sin(\theta_+^V[k])\right)\\ &+\sin^{-1}\left(\sin(\theta_+^H[k])\sin(-\theta_-^V[k])\right)\\ &+\sin^{-1}\left(\sin(-\theta_-^H[k])\sin(-\theta_-^V[k])\right), \quad (6)\end{aligned}$$

which is then logarithmically averaged over a specified frequency range to yield an average CD coverage solid

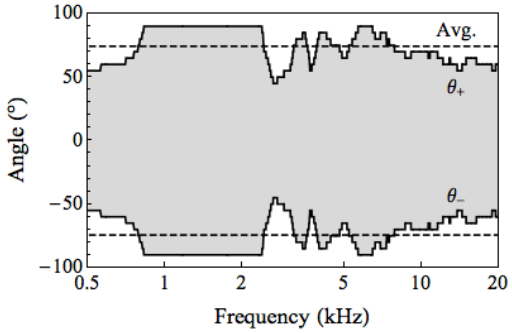

(a) Loudspeaker C: $\overline{\theta_{CD}} = 148.6°$

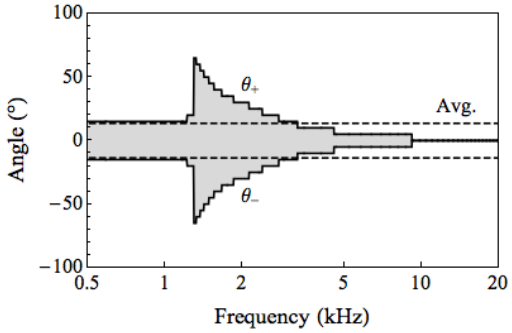

(b) Loudspeaker D: $\overline{\theta_{CD}} = 27.2°$

Fig. 3: Plots of $\theta_-[k]$, $\theta_+[k]$, and $\overline{\theta_{CD}}$ (the difference between the dashed lines) for two loudspeakers, C (top panel) and D (bottom).

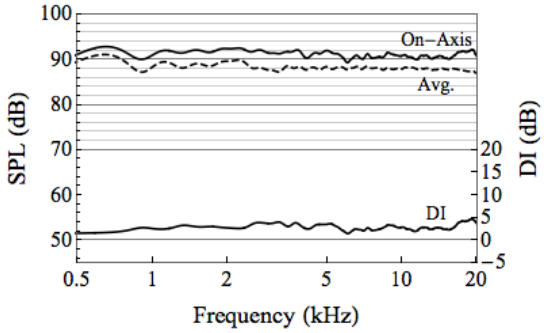

(a) Loudspeaker C: $\overline{\mathrm{DI}} = 2.84$ dB; $\sigma_{\mathrm{DI}} = 0.69$ dB

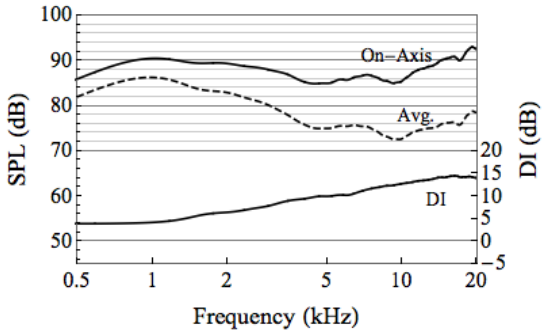

(b) Loudspeaker D: $\overline{\mathrm{DI}} = 8.54$ dB; $\sigma_{\mathrm{DI}} = 3.64$ dB

Fig. 4: Plots of the on-axis and average power spectra, as well as the DI spectra, all in dB, for two loudspeakers, C (top panel) and D (bottom).

angle, $\overline{\Omega_{CD}}$. Note that values for Ω_{CD} will range from 0 to 2π sr because we restrict the original angle calculations to the region of space in front of the transducer.

3.4 Metric 4: Standard Deviation of Directivity Index

For this metric, we compute the logarithmically-weighted standard deviation (see Appendix for details) of the directivity index (DI) spectrum of a transducer, which is defined as the ratio of the on-axis power spectrum to the average power spectrum over all directions, and is given in dB by

$$\mathrm{DI}[k] = 10\log_{10}\frac{|H_0[k]|^2}{\sum_{n=0}^{N-1} w_n |H_n[k]|^2 / \sum_{n=0}^{N-1} w_n}, \quad (7)$$

where w_n are the weights mentioned in Section 3.2 and N is now the total number of measured power spectra. These weights are given by Tylka and Choueiri [13], and correspond to the surface area of the unit sphere represented by each measurement. For partial sections of the polar radiation patterns (e.g., forward horizontal radiation alone), we use the *partial DI spectra* as defined by Tylka and Choueiri [13], which allow certain sections of the radiation pattern to be isolated when evaluating directivity. In the case of the standard full-sphere DI, the calculation in Eq. (7) is equivalent to that proposed by Wilson [14, 15], which is itself equivalent to the graphical method proposed by Kendig and Mueser [7].

The standard deviation, σ_{DI}, quantifies the extent to which the transducer's directivity is constant with frequency, with $\sigma_{\mathrm{DI}} = 0$ indicating that the DI is invariant with frequency. However, as discussed in Section 2, this does not adhere to the strictest definition of constant directivity, as a small σ_{DI} means only that the ratio between the on-axis and the average power spectrum remains nearly constant with frequency – the polar

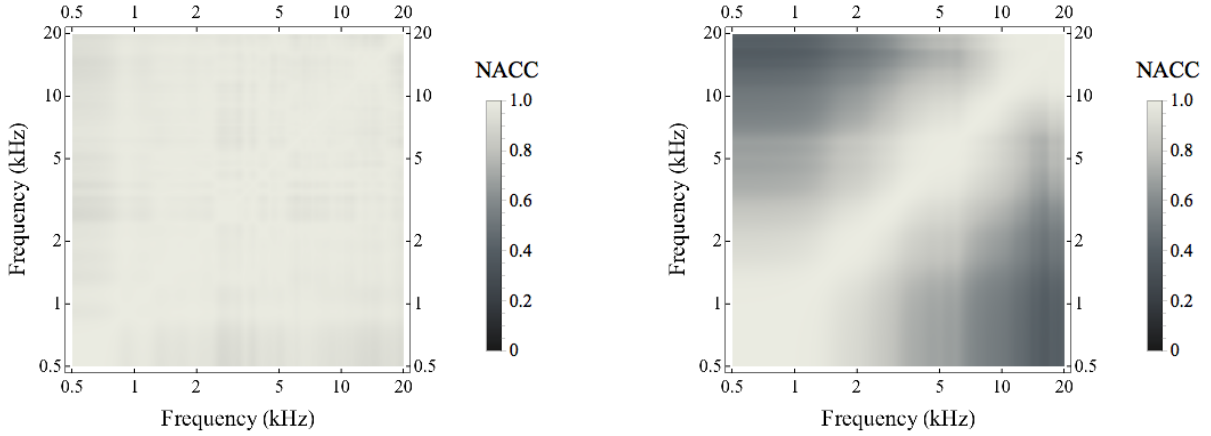

(a) Loudspeaker C: $\overline{\overline{\Phi}} = 0.98$ **(b)** Loudspeaker D: $\overline{\overline{\Phi}} = 0.79$

Fig. 5: Normalized and aligned cross-correlation (NACC) matrices for two loudspeakers, C (left panel) and D (right).

radiation pattern may still vary with frequency.

Figure 4 shows plots of the on-axis and average power spectra, as well as the DI spectra, all in dB, for the two loudspeakers C and D. The large variation in the DI spectrum for loudspeaker D, compared to that of C, yields a larger σ_{DI} value, indicating that loudspeaker D is less constant-directive than loudspeaker C.

3.5 Metric 5: Cross-Correlation of Polar Responses

We define the normalized and aligned cross-correlation (NACC), $\Phi[k_i, k_j]$, between two polar responses at frequency indices k_i and k_j as

$$\Phi[k_i,k_j] = \frac{\sum_{n=0}^{N-1} P_n[k_i]P_n[k_j]}{\left(\sum_{n=0}^{N-1} P_n^2[k_i] \sum_{n=0}^{N-1} P_n^2[k_j]\right)^{0.5}}, \qquad (8)$$

for $k_i, k_j \in [0, K/2]$, where K is the number of points in each power spectrum (and so $K/2$ corresponds to the Nyquist frequency), $P_n[k]$ is the n^{th} power spectrum as before, and N is again the total number of power spectra. Using the above definition for Φ, we compute the NACC between pairs of polar responses for every combination of frequencies. For each frequency pair (k_i, k_j), we then have one NACC value. We then write $\Phi[k_i, k_j]$ as a square matrix with $K/2+1$ rows and columns, where all elements along the main diagonal are always equal to unity and the matrix is necessarily symmetric. This matrix is visualized as shown in Fig. 5 for the same loudspeakers, C and D, as before. We see, for both plots, that the NACC values along the diagonal from the bottom left to the top right corners of each plot are identically 1 (indicated by the white color). Furthermore, since the plot for loudspeaker C is largely white, whereas that for loudspeaker D has significant regions of low NACC values (indicated by the black color), we again conclude that loudspeaker C is more constant-directive than D.

We also compute an average NACC value by computing a logarithmically-weighted mean over a specified range of frequencies, first across columns and then across rows. This average value, $\overline{\overline{\Phi}}$, can take any value between 0 and 1, with a value of 1 indicating that the transducer's polar responses in that frequency range are all identical.

4 Experimental Evaluation of Metrics

To evaluate the metrics proposed in the previous section, we apply the metrics to a database of loudspeaker polar radiation measurements. This database contains measurements made by the authors as part of an ongoing experimental survey of loudspeaker directivity and, at the time of writing, consists of 26 loudspeakers of various types [16]. The data are available as anechoic

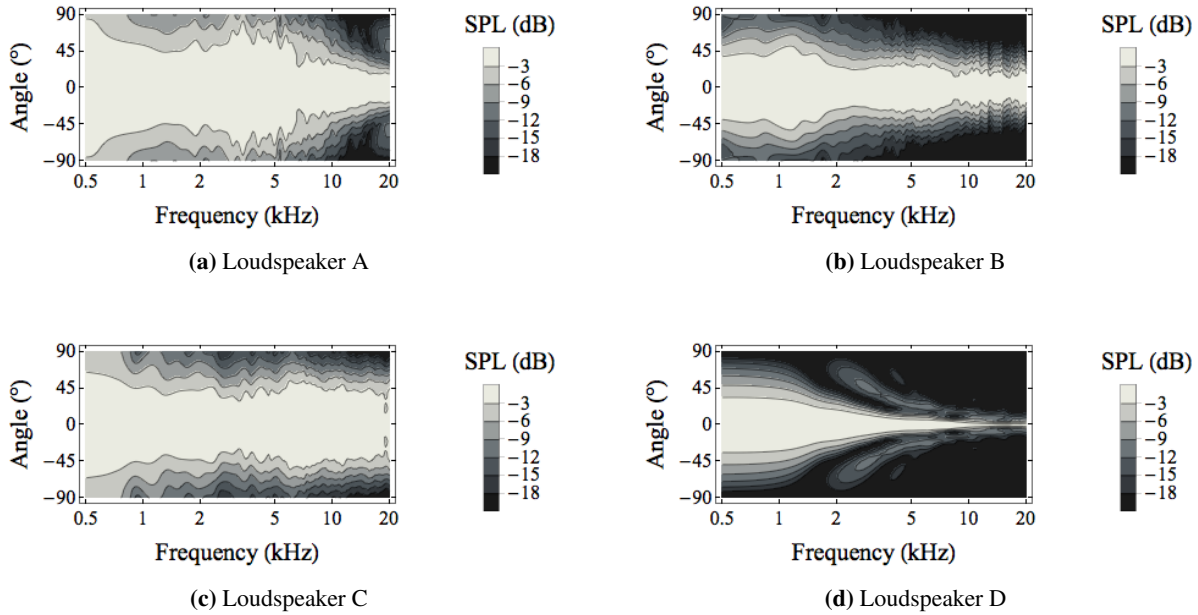

(a) Loudspeaker A

(b) Loudspeaker B

(c) Loudspeaker C

(d) Loudspeaker D

Fig. 6: Contour plots of forward horizontal radiation for the four loudspeakers described in Table 1. Each plot shows SPL normalized by the respective loudspeaker's on-axis response.

impulse responses measured along horizontal and vertical orbits around each loudspeaker, with an angular resolution of 5°. For simplicity, we select and analyze four loudspeakers, whose descriptions are provided, in brief, in Table 1. The metrics proposed here have also been computed and published online for the entire database (see footnote 1 on page 2).

We compute each metric using the forward horizontal radiation data of each selected loudspeaker, contour plots of which are shown in Fig. 6. We then rank the loudspeakers according to their calculated values for each metric, and subsequently evaluate the metrics through comparison with the contour plots. Note that because we only use forward horizontal radiation data, we do not compute the constant-directive coverage solid angle. For metric 1, we generate contour plots over the frequency range from 500 Hz to 20 kHz, with contour lines drawn from -3 dB to -18 dB in increments of 3 dB, and convert the plot to an image with a width of $V = 64$ pixels and a height of $U = 32$ pixels.[4] For metric 2, we define the listening window as $\pm 30^\circ$ from on-axis. For metric 3, we use a distortion threshold of 3 dB. All frequency-domain averages are performed over the range 500 Hz to 20 kHz.

5 Results and Discussion

The calculated values for each metric and for each loudspeaker are tabulated in Table 2, and the rankings, from most constant-directive to least, according to each metric, are shown in Table 3.

We observe that metric 1 differs from the other four metrics in that it is the only metric that ranks loudspeaker D above A. This is likely because this metric places too much weight on the contour plot having sections of the contours that are strictly horizontal. It appears unable, however, to accurately assess the extent to which a loudspeaker is constant-directive over the *entire* frequency range (500 Hz to 20 kHz in this case). Therefore, even though the main lobe of loudspeaker D narrows (and hence its directivity increases) dramatically above 2 kHz, its contour lines are largely horizontal above and below that point, resulting in a higher ranking than for

[4] We intentionally choose such a low-resolution image so as to "blur" the contour lines, thereby reducing the sensitivity of the computed metric to minor fluctuations in the contour lines. Furthermore, we expect this to correspond better with evaluations of constant directivity based on a purely visual analysis of the contour plot, because such an analysis is likely to involve a certain amount of visual averaging.

loudspeaker A, whose contours are rarely horizontal, but whose overall directivity varies less significantly (see Figs. 6a and 6d).

We also see that metrics 4 and 5 generate the same ranking, which is different from that generated by both 2 and 3. The difference is that these latter metrics (both based on criterion II) rank loudspeaker A above B, likely because the width of the main lobe is consistently larger for A than it is for B (as shown by the white regions in Figs. 6a and 6b), resulting in generally smaller distortions of near-to-on-axis frequency responses for loudspeaker A. We also observe an apparent discrepancy between metrics 2 and 3 indicated by the comparable values of $\overline{C_{\mathrm{LW}}}$ for loudspeakers A, B, and C, but the significant difference between the value of $\overline{\theta_{\mathrm{CD}}}$ for loudspeaker B, and those for A and C. However, as all of the $\overline{\theta_{\mathrm{CD}}}$ values are well over 60° (recall that we average the distortion spectra over ±30° to calculate $\overline{C_{\mathrm{LW}}}$), the consistently low (< 1 dB) values of $\overline{C_{\mathrm{LW}}}$ for A, B, and C are to be expected. Metrics 4 and 5 (both based on criterion III), not only rank the loudspeakers in the same order, but also have values that exhibit a similar trend (see Table 2). In view of the discussion regarding criterion III in Section 2, this agreement between the highly constant-directive loudspeakers (A, B, and C) suggests that a high correlation of polar responses guarantees a low standard deviation of directivity index.

Based on a visual comparison of the four contour plots shown in Fig. 6 with each other (and with the contour plot of an "ideal" constant-directive loudspeaker shown in Fig. 1), we expect loudspeaker D to be significantly less constant-directive than the other three loudspeakers due to a significant increase in its directivity with frequency. Furthermore, the prominent high-frequency (> 15 kHz) side-lobes, and larger variation (with frequency) in the main lobe width for loudspeaker A suggest that it is less constant-directive than both B and C. As this ranking order (C, B, A, and D) is obtained only by metrics 4 and 5, we conclude that these metrics are likely the most effective indicators of constant directivity. This conclusion is somewhat surprising, as the standard deviation of directivity index is based on the more lenient version of the third criterion, while the cross-correlation of polar responses is based on the more strict version.

Label	ε (%)	$\overline{C_{\mathrm{LW}}}$ (dB)	$\overline{\theta_{\mathrm{CD}}}$ (°)	σ_{DI} (dB)	$\overline{\overline{\Phi}}$
A	42.79	0.68	141.0	1.57	0.94
B	51.20	0.84	102.8	1.31	0.96
C	55.52	0.38	148.6	0.69	0.98
D	43.65	12.36	27.2	3.64	0.79

Table 2: Calculated values of the five constant directivity metrics for each of the four loudspeakers (labeled A–D) used in this analysis.

Rank	ε	$\overline{C_{\mathrm{LW}}}$	$\overline{\theta_{\mathrm{CD}}}$	σ_{DI}	$\overline{\overline{\Phi}}$
1	C	C	C	C	C
2	B	A	A	B	B
3	D	B	B	A	A
4	A	D	D	D	D

Table 3: The four loudspeakers (labeled A–D) used in this analysis ranked, from most constant-directive to least, according to each of the five metrics.

6 Conclusions

Motivated by the lack of a precise, standardized definition of constant directivity, and of metrics that quantify the extent to which a transducer exhibits constant directivity, we derived a set of five metrics, each of which satisfy one or more of three criteria for constant directivity specified in Section 2. These criteria were also used to define the term "constant directivity" as either a characteristic of a transducer whose polar radiation patterns are invariant across a specified range of frequencies, or, more leniently, as a transducer whose directivity factor (index) is invariant with frequency.

The first metric we proposed involves a Fourier analysis of contour lines (i.e., lines of constant sensitivity over frequency and angle), and is based on the first criterion for constant directivity which requires that a transducer exhibiting constant directivity (i.e., a constant-directive transducer) have a contour plot with all contour lines perfectly horizontal. The second and third metrics are based on the second criterion which requires that constant-directive transducers demonstrate minimal distortion in their off-axis frequency response. These metrics were computed by averaging frequency

response distortions over a range of directions (metric 2) and by distortion thresholding polar responses to determine an angular region of low-distortion (metric 3). The fourth and fifth metrics are based on the third criterion, which requires that the directivity of the transducer be invariant with frequency, or more strictly, that the polar radiation pattern of the transducer remain unchanged with frequency, with satisfaction of the latter variant guaranteeing satisfaction of the former (see Section 2). These metrics were computed by taking the standard deviation of the directivity index (metric 4) and averaging the normalized and aligned cross-correlation (NACC) of polar responses (metric 5).

To evaluate these metrics, we used measured forward horizontal polar radiation data of four loudspeakers, the details of which are presented in Section 4 (also see Table 1). We then ranked, from most to least constant-directive, the four loudspeakers according to each of the five metrics (see Table 3). We found, in general, that metrics derived based on the same criterion for constant directivity produced similar results when quantifying the extent to which the four loudspeakers exhibit constant directivity. Furthermore, by informally comparing the rankings generated by each of the five metrics, and that determined based on a visual comparison of the four contour plots shown in Fig. 6, we found that the standard deviation of the directivity index and the average NACC are likely the best indicators of the extent to which a transducer exhibits constant directivity.

All five metrics presented in this work were derived only for a single polar orbit, with the exception of the constant directivity coverage solid angle, which requires both a horizontal and a vertical polar orbit (see Section 3.3). Consequently, a useful extension to the work in this paper would be to compute similar metrics using full, three-dimensional polar radiation data, which is becoming increasingly available and is prescribed in the AES standard on polar radiation measurements [17]. For instance, instead of computing the NACC of polar responses belonging to a single polar orbit as discussed in Section 3.5, one might compute an equivalent two-dimensional NACC where a three-dimensional polar radiation pattern at a given frequency (represented mathematically by a matrix of polar responses) is cross-correlated with another such polar radiation pattern at a different frequency. This and other three-dimensional constant directivity metrics would enable a more complete analysis of measured polar radiation patterns of transducers. Although not explicitly considered here, we expect these metrics to be applicable to many types of transducers, including microphones and arrays (of loudspeakers or of microphones).

Acknowledgements

This work is sponsored by the Sony Corporation of America.

Appendix: Logarithmically-Weighted Mean and Variance

Consider a discrete spectrum $X[k]$ for $k \in [0, K-1]$, where the frequency index, k, is proportional to the frequency in Hz, given by kF_s/K, and F_s is the sampling rate. We define the logarithmic average, $\overline{X}$, over the frequency index range $[K_1, K_2]$, as a weighted average

$$\overline{X} = \frac{\sum_{k=K_1}^{K_2} W[k] \cdot X[k]}{\sum_{k=K_1}^{K_2} W[k]}, \tag{9}$$

where the weights W are given by

$$W[k] = \log \frac{k+0.5}{k-0.5}. \tag{10}$$

Similarly, we define the logarithmic variance σ_X^2 by

$$\sigma_X^2 = \frac{\sum_{k=K_1}^{K_2} W[k] \left(X[k] - \overline{X}\right)^2}{\sum_{k=K_1}^{K_2} W[k]}. \tag{11}$$

References

[1] White, J., "The Constant Directivity White Horn White Paper," in *The PA Bible*, Addition 6, Electro-Voice, Inc., 1980.

[2] Van der Wal, M., Start, E. W., and de Vries, D., "Design of Logarithmically Spaced Constant-Directivity Transducer Arrays," *J. Audio Eng. Soc.*, 44(6), pp. 497–507, 1996.

[3] Ward, D. B., Kennedy, R. A., and Williamson, R. C., "Constant Directivity Beamforming," in M. Brandstein and D. Ward, editors, *Microphone Arrays: Signal Processing Techniques and Applications*, chapter 1, pp. 3–17, Springer Berlin Heidelberg, 2001.

[4] Geddes, E., "Directivity in Loudspeaker Systems," GedLee, LLC White Paper, 2009.

[5] Davis, D., Patronis, E., Jr., and Brown, P., *Sound System Engineering*, Focal Press, fourth edition, 2013.

[6] Molloy, C. T., "Calculation of the Directivity Index for Various Types of Radiators," *The Journal of the Acoustical Society of America*, 20(4), pp. 387–405, 1943.

[7] Kendig, P. M. and Mueser, R. E., "A Simplified Method for Determining Transducer Directivity Index," *The Journal of the Acoustical Society of America*, 19(4), pp. 691–694, 1947.

[8] Davis, D., "A Proposed Standard Method of Measuring the Directivity Factor "Q" of Loudspeakers Used in Commercial Sound Work," *J. Audio Eng. Soc.*, 21(7), pp. 571–578, 1973.

[9] Gerzon, M. A., "Calculating the Directivity Factor γ of Transducers from Limited Polar Diagram Information," *J. Audio Eng. Soc.*, 23(5), pp. 369–373, 1975.

[10] Davis, D., "Establishing a Loudspeaker's Directivity Figure of Merit (DFM)," in *Audio Engineering Society Convention 54*, 1976.

[11] Geddes, E. R., "Source Radiation Characteristics," *J. Audio Eng. Soc.*, 34(6), pp. 464–478, 1986.

[12] Devantier, A., "Characterizing the Amplitude Response of Loudspeaker Systems," in *Audio Engineering Society Convention 113*, 2002.

[13] Tylka, J. G. and Choueiri, E. Y., "On the Calculation of Full and Partial Directivity Indices," Technical report, 3D Audio and Applied Acoustics Laboratory, Princeton University, 2014.

[14] Wilson, G. L., "Directivity Factor: Q or R_θ? Standard Terminology and Measurement Methods," *J. Audio Eng. Soc.* (Forum), 21(10), pp. 828, 830, 833, 1973.

[15] Wilson, G. L., "More on the Measurement of the Directivity Factor," *J. Audio Eng. Soc.* (Forum), 22(3), pp. 180, 182, 1974.

[16] Tylka, J. G., Sridhar, R., and Choueiri, E. Y., "A Database of Loudspeaker Polar Radiation Measurements," in *Audio Engineering Society Convention 139*, 2015.

[17] "AES56-2008: AES standard on acoustics - Sound source modeling - Loudspeaker polar radiation measurements," 2008 (reaffirmed 2014).